had associated Graves' disease preoperatively, and were strictly followed up after surgery in our institutes. All 4 patients underwent STA-MCA anastomosis with encephalo-duro-myo-synangiosis (EDMS) and dural pedicle insertion[14] during the euthyroid state. Surgical criteria for moyamoya disease in our institute include presence of ischemic symptom, apparent hemodynamic compromise, activity of daily living better than modified Rankin scale 2, and absence of major cerebral infarction. Preoperative CBF and cerebral hemodynamic reserve capacity (CVR) were assessed using a stimulated CBF study with or without acetazolamide loading using *N*-isopropyl-p-[^{123}I]iodoamphetamine single-photon emission computed tomography (^{123}I-IMP SPECT). Postoperative CBF was routinely measured by ^{123}I-IMP SPECT 1 and 7 days after surgery. Magnetic resonance (MR) imaging and MR angiography were performed 2 and 8 days after surgery. Graves' disease was suspected when the patients showed typical clinical symptoms such as bilateral exophthalmos, diffuse goiter or dermopathy at initial presentation, and the diagnosis was made by an endocrinologist. In all 4 patients, levels of thyroid-stimulating hormone, free triiodothyronine (T3), and free thyroxine (T4) were tested at initial presentation to our hospital and in the perioperative period.

Results

The clinical features of the 4 Japanese patients (1 male and 3 females) aged from 34 to 55 years (mean 41.8 years) are summarized in Table 1. All patients initially presented with transient ischemic attack (TIA). Three patients (Cases 2, 3, and 4) presented with TIA and one patient (Case 1) presented with intracerebral hemorrhage. Two patients (Cases 2 and 4) were diagnosed with moyamoya disease and Graves' disease at the same time at the first visit. Case 1 had been diagnosed with moyamoya disease based on TIA prior to the diagnosis of Graves' disease, and presented with intracerebral hemorrhage 10 years after the initial diagnosis of moyamoya disease. Case 3 had been diagnosed with Graves' disease 30 years prior to the diagnosis of moyamoya disease based on progressive TIA.

Thyroid function for each patient is summarized in Table 2. Three of the 4 patients (Cases 2, 3, and 4) presented with thyrotoxic crisis, and one patient (Case 1) with moderate hyperthyroidism (Table 2). Hyperthyroidism was treated with thiamazole for 2

Table 1 Summary of the present cases

Case No.	Age (yrs)/ Sex	Age (yrs) at diagnosis of		Pattern of symptom	Angiographical lesions	Neuroimaging findings	
		Hyperthyroidism	Moyamoya disease			Preoperative SPECT, CT, or MR imaging	Postoperative SPECT or MR imaging
1	42/F	36	32	TIA→ICH	bil	decreased CBF & CVR (rt), ICH at caudate nucleus (rt)	increased CBF, no ischemic lesion
2	36/M	36	36	TIA	bil	decreased CBF (rt) & CVR (bil), previous infarction (rt watershed)	increased CBF, no ischemic lesion
3	55/F	20	53	TIA	lt	decreased CBF & CVR (lt), chronic ischemic change (lt)	increased CBF, no ischemic lesion
4	34/F	34	34	TIA	bil	decreased CBF & CVR (rt), chronic ischemic change (rt)	increased CBF, no ischemic lesion

CBF: cerebral blood flow, CVR: cerebrovascular reserve capacity, ICH: intracerebral hemorrhage, TIA: transient ischemic attack.

Table 2 Thyroid function of the present cases

Case No.	Initial value*			Preoperative value		
	Free T3 (pg/dl)	Free T4 (ng/dl)	TSH (mU/ml)	Free T3 (pg/dl)	Free T4 (ng/dl)	TSH (mU/ml)
1	6.67	2.70	<0.01	2.27	0.80	<0.01
2	29.9	8.16	0.05	3.38	1.09	0.05
3	30.0	6.00	0.03	5.01	1.69	0.05
4	22.4	8.71	0.05	2.65	0.44	0.05

*Initial value was obtained from the test performed on first presentation to our institution.

to 3 months in all patients. The frequency of cerebral ischemic symptoms decreased after the antithyroid treatment. STA-MCA anastomosis was performed when the patients were euthyroid (Table 2). Antithyroid medications were restarted from the next day after surgery, and euthyroid was maintained during perioperative period in all patients.

The preoperative neuroimaging findings are summarized in Table 1. One patient (Case 1) had intracerebral hemorrhage at the right caudate nucleus with intraventricular hematoma on computed tomography. The other 3 patients (Cases 2, 3, and 4) had some sort of ischemic change including previous cerebral infarction (Case 2) on MR imaging. Three of the 4 patients (Cases 1, 2, and 4) had bilateral stenoocclusive changes on cerebral angiography, and one patient (Case 3) had unilateral lesions. All patients had decreased CBF and significantly impaired CVR on ^{123}I-IMP SPECT.

Revascularization surgery was performed for the 5 affected hemispheres; unilateral in 3 patients (Cases 1, 3, and 4) and bilateral for 1 patient (Case 2). Second revascularization was performed 6 months after the initial surgery in Case 2. Postoperative SPECT revealed increase in CBF in the side of revascularization in all patients (Table 1). The patency of STA-MCA bypass was confirmed in all patients by postoperative MR angiography. Postoperative MR imaging showed no ischemic or hemorrhagic complications.

One patient (Case 2) complained of frequent headaches on postoperative day 3, and developed transient fluctuating aphasia on postoperative day 5. These symptoms were considered to be due to cerebral hyperperfusion based on the postoperative CBF analysis and blood pressure dependency of the symptom. Intensive blood pressure control by nicardipine relieved these symptoms, which completely disappeared 15 days after surgery. Postoperative courses of the other 3 patients (Cases 1, 3, and 4) were uneventful, and all patients were discharged within 20 days after surgery. All patients returned to normal daily life, and no ischemic attack occurred during the follow-up period.

Representative Case 4: A 34-year-old female presented with crescendo transient motor weakness in her left upper extremity. Initial MR imaging revealed slight chronic ischemic changes in the right cerebral hemisphere (Fig. 1A). Cerebral angiography showed right-side dominant steno-occlusive changes (Fig. 1B, C). Preoperative SPECT showed slightly decreased CBF (Fig. 2) and significantly impaired CVR in the right middle cerebral artery territory (not shown). Physical examination revealed bilateral exophthalmos and goiter. High-titer thyroid-stimulating hormone receptor antibodies were detected and thyroid function tests revealed thyrotoxicosis (Table 2). The patient was diagnosed with Graves' disease by an endocrinologist.

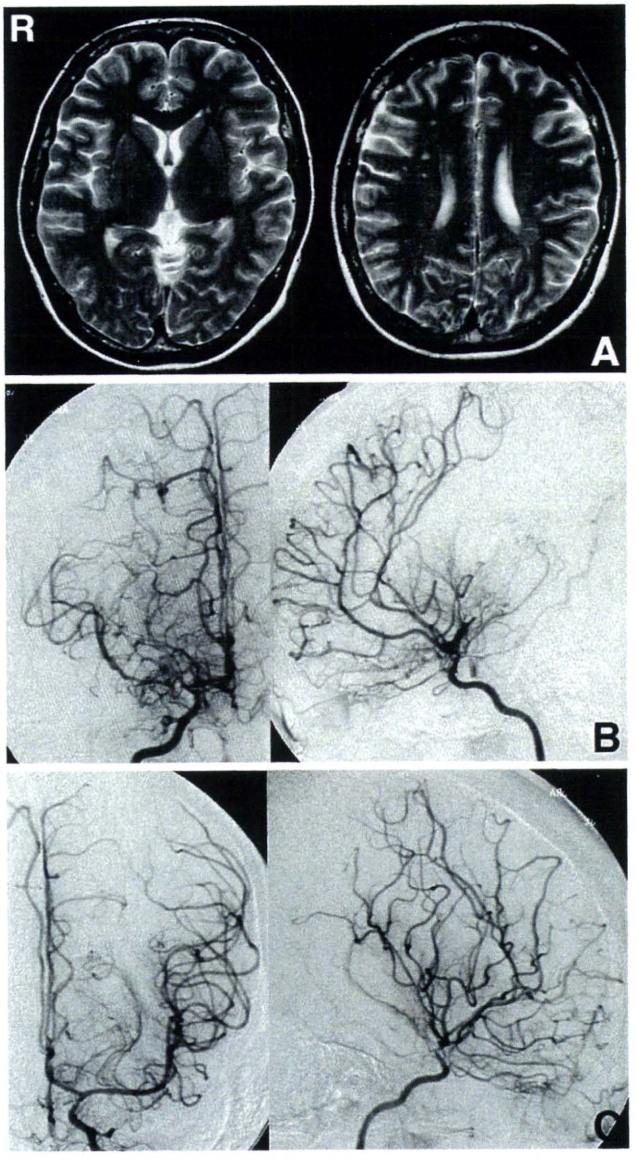

Fig. 1 Case 4. A: Preoperative T_2-weighted magnetic resonance images revealing multiple spotty high intensity lesions in the deep white matter of right cerebral hemisphere. B: Right carotid angiograms revealing mild stenosis at the terminal portion of the right internal carotid artery and proximal portion of the right anterior cerebral artery. Right middle cerebral artery was occluded at its origin and reconstructed by net-like collateral vessels. C: Left carotid angiograms showing mild stenotic change at the terminal portion of the left internal carotid artery.

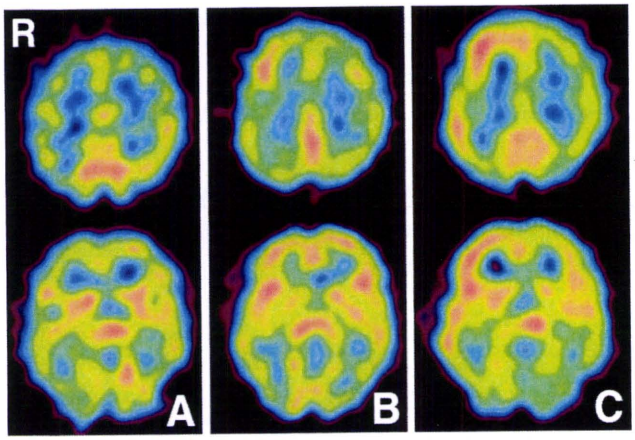

Fig. 2 Case 4. *N*-isopropyl-p-[^{123}I]iodoamphetamine single-photon emission computed tomography scans before (A) and 1 (B) and 7 days (C) after surgery showing increased cerebral blood flow in the operated hemisphere, especially on day 7.

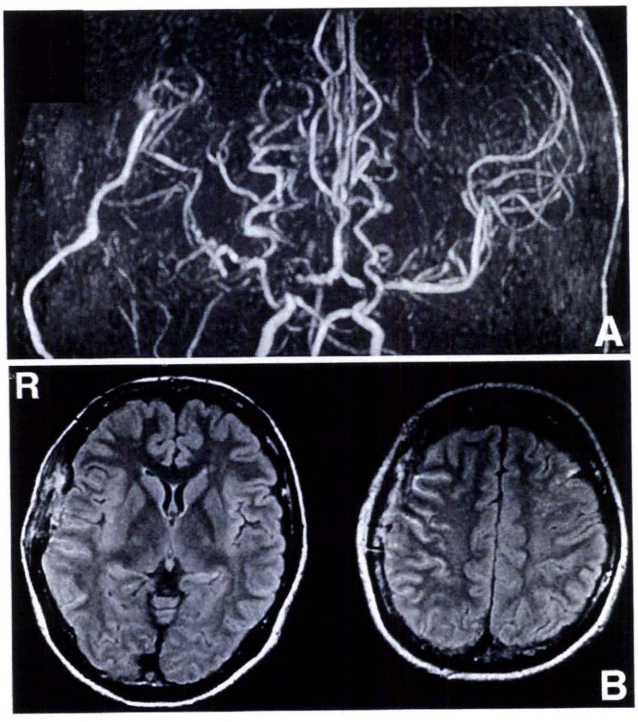

Fig. 3 Case 4. A: Magnetic resonance angiogram performed 8 days after surgery revealing the patent superficial temporal artery-middle cerebral artery bypass. B: Fluid-attenuated inversion recovery magnetic resonance images showing no perioperative ischemic complication.

The frequency of the TIAs gradually decreased during 2 months treatment with thiamazole. Right STA-MCA anastomosis with EDMS and dural pedicle insertion was performed when the patient was euthyroid. Euthyroid was maintained through perioperative period by anti-thyroid treatment. Postoperative SPECT on days 1 and 7 revealed increased CBF in the right cerebral hemisphere (Fig. 2). Her blood pressure was strictly controlled between 100 and 140 mmHg to prevent symptomatic cerebral hyperperfusion and cerebral ischemia until discharge. Postoperative MR imaging on days 2 and 8 showed no ischemic or hemorrhagic complications with the patent STA-MCA anastomosis (Fig. 3). The patient was discharged 11 days after surgery, and the ischemic attack never recurred after discharge.

Discussion

The mechanisms underlying the rare combination of moyamoya vasculopathy and Graves' disease remain undetermined. Hereditary and immunogenic inflammatory factors have been implicated in the etiology of moyamoya disease. Histological analysis of intracranial vessels in moyamoya disease has revealed subendothelial fibrous tissue occluding the vascular lumen, intimal thickening, and smooth muscle cell proliferation, and the presence of macrophages and T cells.[11] The cellular proliferation and vascular dysregulation in moyamoya disease and immunologic stimulation of the thyroid in Graves' disease may have a common pathogenic link involving T-cell dysregulation.[17,19] In addition to these mechanical vascular abnormalities, excessive thyroid hormones may affect cerebral metabolism, cerebral oxygen consumption, cerebral hemodynamics, and cerebrovascular autoregulation, which may be triggers of the cerebral ischemic event.[7,9,10,19] The effectiveness of simple antithyroid therapy for cerebral ischemic symptoms might indirectly prove these mechanisms. Further study is required to obtain more evidence of the relationship between genetic and immunogenic backgrounds for these associated conditions.

We treat symptomatic patients with moyamoya disease by STA-MCA anastomosis with EDMS and dural pedicle insertion. We applied this treatment strategy to our patients with moyamoya syndrome associated with Graves' disease, and successfully performed revascularization. Whether the present cases should be simply recognized as a symptomatic group remains unclear, because the cerebral ischemic symptoms were relieved by antithyroid treatment. A total of 23 cases including

Table 3 Summary of reported cases

Author (Year)	Age (yrs)/ Sex	Onset	Thyroid condition at onset	Treatment	Outcome
Kushima et al. (1991)[9]	21/F	infarction	thyrotoxic state	antithyroid therapy	GR
	22/F	infarction	thyrotoxic state	antithyroid therapy	ND
Matsumoto et al. (1992)[12]	35/F	infarction	thyrotoxic state	antithyroid therapy	MD
Liu et al. (1994)[10]	28/F	infarction	thyrotoxic state	antithyroid therapy	ND
Tendler et al. (1997)[19]	37/F	infarction	thyrotoxic state	antithyroid therapy	GR
	38/F	ND	thyrotoxic state	antithyroid therapy	GR
Wakamoto et al. (2000)[21]	19/F	hemorrhage	thyrotoxic state	antithyroid therapy	GR
Nakamura et al. (2003)[13]	23/F	infarction	thyrotoxic state	antithyroid therapy/STA-MCA + EMS	GR
	54/F	infarction	upper limit	antithyroid therapy/STA-MCA + EMS	GR
Utku et al. (2004)[20]	45/F	TIA	thyrotoxic state	antithyroid therapy	GR
Im et al. (2005)[7]	22/F	infarction	thyrotoxic state	antithyroid therapy/STA-MCA + EMS	GR
	22/F	infarction	thyrotoxic state	antithyroid therapy/EDAS	GR
	22/F	infarction	thyrotoxic state	antithyroid therapy/STA-MCA + EMS	GR
	25/F	infarction	thyrotoxic state	antithyroid therapy/STA-MCA + EDAS	GR
Golomb et al. (2005)[5]	10/F	infarction	thyrotoxic state	antithyroid therapy/pial synangiosis	GR
Hsu et al. (2006)[6]	40/F	infarction	thyrotoxic state	conservative	D
Sasaki et al. (2006)[16]	27/F	TIA	thyrotoxic state	antithyroid therapy/EDAS	GR
	36/F	infarction	thyrotoxic state	antithyroid therapy	GR
	16/F	infarction	thyrotoxic state	antithyroid therapy/EDAS	GR
Present Cases 1	42/F	TIA/hemorrhage	moderate hyperthyroidism	antithyroid therapy/STA-MCA + EDMS	GR
Present Case 2	36/M	TIA/infarction	thyrotoxic state	antithyroid therapy/STA-MCA + EDMS	GR
Present Case 3	55/F	TIA	thyrotoxic state	antithyroid therapy/STA-MCA + EDMS	GR
Present Case 4	34/F	TIA	thyrotoxic state	antithyroid therapy/STA-MCA + EDMS	GR

D: dead, EDAS: encephalo-duro-arterio-synangiosis, EDMS: encephalo-duro-myo-synangiosis, EMS: encephalo-myo-synangiosis, GR: good recovery, MD: moderate disability, ND: not described, STA-MCA: superficial temporal artery-middle cerebral artery anastomosis, TIA: transient ischemic attack.

the present cases of moyamoya vasculopathy associated with Graves' disease have been described (Table 3).[5-7,9,10,12,13,16,19-21] Interestingly, most of these cases were thyrotoxic when the cerebral ischemic symptoms developed. Thirteen of these patients were successfully treated with antithyroid therapy followed by revascularization surgery. In contrast, ischemic symptoms were successfully controlled only with antithyroid therapy in some patients, although the long-term outcomes after the medical treatment were unclear.[9,19-21] The overall relapse rate of Graves' disease after effective antithyroid therapy is as high as 50%.[15] Relapse of the hyperthyroidism would affect the remission of the cerebral ischemic symptoms. Indeed, 2 cases of this study (Cases 1 and 3) were admitted with recurrent hyperthyroid state during medical treatment for Graves' disease. Moreover, atherosclerotic changes of the cerebral blood vessels with aging facilitate decreased CBF, because most of the cases are adult-onset moyamoya syndrome. Therefore, prophylactic revascularization for moyamoya vasculopathy with Graves' disease to reduce the potential risk of cerebral ischemic injury can be justified, even if the patients are relieved from ischemic symptoms after antithyroid therapy. The effects of presurgical antithyroid therapy on CBF and CVR capacities may need to be investigated to determine the surgical indications. The major premise for revascularization surgery is optimal remission of hyperthyroidism throughout the perioperative period. Nine previous patients were surgically treated after medical therapy for hyperthyroidism, of whom one developed postoperative ischemic brain injury.[7]

In this series, revascularization was performed without remission of thyrotoxicosis. We restarted administration of antithyroid agent from the day after surgery to maintain the euthyroid state, and no patient suffered postoperative ischemic complication. There is little evidence for the effectiveness of presurgical usage of antiplatelet combined with antithyroid agents for the prevention of cerebral ischemia. Careful administration of antiplatelet agent would be required, considering the inclusion of hemorrhagic onset cases in our series (Case 1). Moyamoya syndrome associated with Graves' disease in children is rare, probably due to the rarity of Graves' disease in children. The need for surgical

treatment for these young patients should be carefully investigated because of the worse prognosis for younger patients with moyamoya disease.[8]

We performed cerebrovascular reconstruction surgery for moyamoya disease, focusing on the cerebral hemodynamics in the early postoperative period.[2,3] Based on our previous studies, postoperative cerebral hyperperfusion is a potential risk of direct revascularization surgery for moyamoya disease.[2,3] Furthermore, we rarely experienced patients with delayed intracerebral hemorrhage caused by postoperative hyperperfusion.[4] In the present study, postoperative SPECT of all 4 patients showed increased CBF in the operated hemisphere compared with preoperative SPECT. One patient (Case 2) developed symptomatic hyperperfusion, which was improved by intensive blood pressure control, which seemed to suggest that the postoperative cerebral hemodynamics of moyamoya syndrome associated with Graves' disease vary similarly to pure moyamoya disease. Therefore, postoperative blood pressure control to avoid both symptomatic ischemia and hyperperfusion would be desirable in addition to perioperative maintenance of the euthyroid state. In the present study, postoperative cerebral hemodynamics and patency of the STA-MCA anastomosis were manifested during early postoperative period. However, long-term patency of the revascularization, especially of the indirect bypass, for moyamoya syndrome associated with Graves' disease is unknown. The development of collateral vessels via the temporal muscle flap as well as patent STA bypass were angiographically confirmed 6 months after surgery.[13] Lengthy follow up by MR angiography and SPECT are required for the present cases to assess the long-term effectiveness of revascularization surgery for this entity.

Cerebrovascular reconstruction surgery is a successful treatment option for moyamoya syndrome associated with Graves' disease. Timing of surgery during the euthyroid state and perioperative management considering thyroid function and cerebral hemodynamic change are the keys to successful surgical treatment.

References

1) Baaj AA, Agazzi S, Sayed ZA, Toledo M, Spetzler RF, van Loveren H: Surgical management of moyamoya disease: a review. *Neurosurg Focus* 26(4): E7, 2009
2) Fujimura M, Kaneta T, Mugikura S, Shimizu H, Tominaga T: Temporary neurologic deterioration due to cerebral hyperperfusion after superficial temporal artery-middle cerebral artery anastomosis in patients with adult-onset moyamoya disease. *Surg Neurol* 67: 273–282, 2007
3) Fujimura M, Mugikura S, Kaneta T, Shimizu H, Tominaga T: Incidence and risk factors for symptomatic cerebral hyperperfusion after superficial temporal artery-middle cerebral artery anastomosis in patients with moyamoya disease. *Surg Neurol* 71: 442–447, 2009
4) Fujimura M, Shimizu H, Mugikura S, Tominaga T: Delayed intracerebral hemorrhage after superficial temporal artery-middle cerebral artery anastomosis in a patient with moyamoya disease: possible involvement of cerebral hyperperfusion and increased vascular permeability. *Surg Neurol* 71: 223–227, 2009
5) Golomb MR, Biller J, Smith JL, Edwards-Brown M, Sanchez JC, Nebesio TD, Garg BP: A 10-year-old girl with coexistent moyamoya disease and Graves' disease. *J Child Neurol* 20: 620–624, 2005
6) Hsu SW, Chaloupka JC, Fattal D: Rapidly progressive fatal bihemispheric infarction secondary to Moyamoya syndrome in association with Graves thyrotoxicosis. *AJNR Am J Neuroradiol* 27: 643–647, 2006
7) Im SH, Oh CW, Kwon OK, Kim JE, Han DH: Moyamoya disease associated with Graves disease: special considerations regarding clinical significance and management. *J Neurosurg* 102: 1013–1017, 2005
8) Kim SK, Seol HJ, Cho BK, Hwang YS, Lee DS, Wang KC: Moyamoya disease among young patients: its aggressive clinical course and the role of active surgical treatment. *Neurosurgery* 54: 840–846, 2004
9) Kushima K, Satoh Y, Ban Y, Taniyama M, Ito K, Sugita K: Graves' thyrotoxicosis and Moyamoya disease. *Can J Neurol Sci* 18: 140–142, 1991
10) Liu JS, Juo SH, Chen WH, Chang YY, Chen SS: A case of Graves' diseases associated with intracranial moyamoya vessels and tubular stenosis of extracranial internal carotid arteries. *J Formos Med Assoc* 93: 806–809, 1994
11) Masuda J, Ogata J, Yutani C: Smooth muscle cell proliferation and localization of macrophages and T cells in the occlusive intracranial major arteries in moyamoya disease. *Stroke* 24: 1960–1967, 1993
12) Matsumoto K, Nogaki H, Yamamoto K, Sasabe F, Morimatsu M: [A case of moyamoya disease complicated with Basedow disease]. *No Socchu* 14: 409–413, 1992 (Japanese)
13) Nakamura K, Yanaka K, Ihara S, Nose T: Multiple intracranial arterial stenoses around the circle of Willis in association with Graves' disease: report of two cases. *Neurosurgery* 53: 1210–1215, 2003
14) Narisawa A, Fujimura M, Tominaga T: Efficacy of the revascularization surgery for adult-onset moyamoya disease with the progression of cerebrovascular lesions. *Clin Neurol Neurosurg* 111: 123–126, 2009
15) Orgiazzi J, Madec AM: Reduction of the risk of relapse after withdrawal of medical therapy for Graves' disease. *Thyroid* 12: 849–853, 2002

16) Sasaki T, Nogawa S, Amano T: Co-morbidity of moyamoya disease with Graves' disease. Report of three cases and a review of the literature. *Intern Med* 45: 649–653, 2006
17) Scott RM, Smith ER: Moyamoya disease and moyamoya syndrome. *N Engl J Med* 360: 1226–1237, 2009
18) Suzuki J, Takaku A: Cerebrovascular "moyamoya" disease. Disease showing abnormal net-like vessels in base of brain. *Arch Neurol* 20: 288–299, 1969
19) Tendler BE, Shoukri K, Malchoff C, MacGillivray D, Duckrow R, Talmadge T, Ramsby GR: Concurrence of Graves' disease and dysplastic cerebral blood vessels of the moyamoya variety. *Thyroid* 7: 625–629, 1997
20) Utku U, Asil T, Celik Y, Tucer D: Reversible MR angiographic findings in a patient with autoimmune Graves disease. *AJNR Am J Neuroradiol* 25: 1541–1543, 2004
21) Wakamoto H, Ishiyama N, Miyazaki H, Shinoda A, Tomita H: [The stenoses at the terminal portion of the internal carotid artery improved after initiation of antithyroid therapy: a case report]. *No Shinkei Geka* 28: 379–383, 2000 (Japanese)

Address reprint requests to: Miki Fujimura, M.D., Ph.D., Department of Neurosurgery, Kohnan Hospital, 4-20-1 Nagamachi-minami, Taihaku-ku, Sendai 982-8523, Japan.
e-mail: fujimur@kohnan-sendai.or.jp

Journal of Human Genetics (2011) 56, 34–40

www.nature.com/jhg

ORIGINAL ARTICLE

A genome-wide association study identifies *RNF213* as the first Moyamoya disease gene

Fumiaki Kamada[1], Yoko Aoki[1], Ayumi Narisawa[1,2], Yu Abe[1], Shoko Komatsuzaki[1], Atsuo Kikuchi[3], Junko Kanno[1], Tetsuya Niihori[1], Masao Ono[4], Naoto Ishii[5], Yuji Owada[6], Miki Fujimura[2], Yoichi Mashimo[7], Yoichi Suzuki[7], Akira Hata[7], Shigeru Tsuchiya[3], Teiji Tominaga[2], Yoichi Matsubara[1] and Shigeo Kure[1,3]

Moyamoya disease (MMD) shows progressive cerebral angiopathy characterized by bilateral internal carotid artery stenosis and abnormal collateral vessels. Although ~15% of MMD cases are familial, the MMD gene(s) remain unknown. A genome-wide association study of 785 720 single-nucleotide polymorphisms (SNPs) was performed, comparing 72 Japanese MMD patients with 45 Japanese controls and resulting in a strong association of chromosome 17q25-ter with MMD risk. This result was further confirmed by a locus-specific association study using 335 SNPs in the 17q25-ter region. A single haplotype consisting of seven SNPs at the *RNF213* locus was tightly associated with MMD ($P=5.3\times10^{-10}$). *RNF213* encodes a really interesting new gene finger protein with an AAA ATPase domain and is abundantly expressed in spleen and leukocytes. An RNA *in situ* hybridization analysis of mouse tissues indicated that mature lymphocytes express higher levels of *Rnf213* mRNA than their immature counterparts. Mutational analysis of *RNF213* revealed a founder mutation, p.R4859K, in 95% of MMD families, 73% of non-familial MMD cases and 1.4% of controls; this mutation greatly increases the risk of MMD ($P=1.2\times10^{-43}$, odds ratio=190.8, 95% confidence interval=71.7–507.9). Three additional missense mutations were identified in the p.R4859K-negative patients. These results indicate that *RNF213* is the first identified susceptibility gene for MMD.
Journal of Human Genetics (2011) **56**, 34–40; doi:10.1038/jhg.2010.132; published online 4 November 2010

INTRODUCTION

'Moyamoya' is a Japanese expression for something hazy, such as a puff of cigarette smoke drifting in the air. In individuals with Moyamoya disease (MMD), there is a progressive stenosis of the internal carotid arteries; a fine network of collateral vessels, which resembles a puff of smoke on a cerebral angiogram, develops at the base of the brain (Figure 1a).[1,2] This steno-occlusive change can cause transient ischemic attacks and/or cerebral infarction, and rupture of the collateral vessels can cause intracranial hemorrhage. Children under 10 years of age account for nearly 50% of all MMD cases.[3]

The etiology of MMD remains unclear, although epidemiological studies suggest that bacterial or viral infection may be implicated in the development of the disease.[4] Growing attention has been paid to the upregulation of arteriogenesis and angiogenesis associated with MMD because chronic ischemia in other disease conditions is not always associated with a massive development of collateral vessels.[5,6] Several angiogenic growth factors are thought to have functions in the development of MMD.[7]

Several lines of evidence support the importance of genetic factors in susceptibility to MMD.[8] First, 10–15% of individuals with MMD have a family history of the disease.[9] Second, the concordance rate of MMD in monozygotic twins is as high as 80%.[10] Third, the prevalence of MMD is 10 times higher in East Asia, especially in Japan (6 per 100 000 population), than in Western countries.[3] Familial MMD may be inherited in an autosomal dominant fashion with low penetrance or in a polygenic manner.[11] Linkage studies of MMD families have revealed five candidate loci for an MMD gene: chromosomes 3p24–26,[12] 6q25,[13] 8q13–24,[10] 12p12–13[10] and 17q25.[14] However, no susceptibility gene for MMD has been identified to date.

We collected 20 familial cases of MMD to investigate linkage in the five putative MMD loci. However, a definitive result was not obtained for any of the loci. We then hypothesized that there might be a founder mutation among Japanese patients with MMD because the prevalence of MMD is unusually high in Japan.[15] Genome-wide and locus-specific association studies were performed and successfully identified a single gene, *RNF213*, linked to MMD. We report here a strong association between MMD onset and a founder mutation in *RNF213*, as well as the expression profiles of *RNF213*, in various tissues.

[1]Department of Medical Genetics, Tohoku University School of Medicine, Sendai, Japan; [2]Department of Neurosurgery, Tohoku University School of Medicine, Sendai, Japan; [3]Department of Pediatrics, Tohoku University School of Medicine, Sendai, Japan; [4]Department of Pathology, Tohoku University School of Medicine, Sendai, Japan; [5]Department of Microbiology and Immunology, Tohoku University School of Medicine, Sendai, Japan; [6]Department of Organ Anatomy, Yamaguchi University Graduate School of Medicine, Ube, Japan and [7]Department of Public Health, Graduate School of Medicine, Chiba University, Chiba, Japan
Correspondence: Dr S Kure, Department of Pediatrics, Tohoku University School of Medicine, 1-1 Seiryo-machi, Aoba-ku, Miyagi, Sendai 980-8574, Japan.
E-mail; kure@med.tohoku.ac.jp
Received 30 September 2010; accepted 1 October 2010; published online 4 November 2010

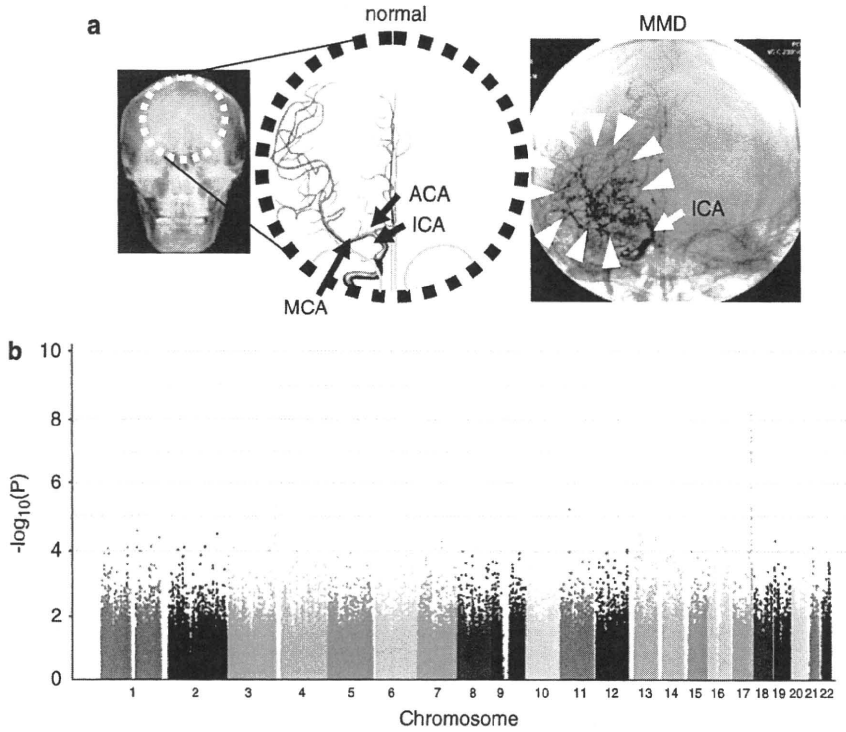

Figure 1 (**a**) Abnormal brain vessels in MMD. The dotted circle indicates the X-ray field of cerebral angiography (left panel). Normal structures of the right internal carotid artery (ICA), anterior cerebral artery (ACA) and middle cerebral artery (MCA) are illustrated (middle panel). The arrowheads indicate abnormal collateral vessels appearing like a puff of smoke in the angiogram of an individual with MMD (right panel). Note that ACA and MCA are barely visible, because of the occlusion of the terminal portion of the ICA. (**b**) Manhattan plot of the 785 720 SNPs used in the genome-wide association analysis of MMD patients. Note that the SNPs in the 17q25-ter region reach a significance of $P<10^{-8}$.

MATERIALS AND METHODS

Affected individuals

Genomic DNA was extracted from blood and/or saliva samples obtained from members of the families with MMD (Supplementary Figure 1), MMD patients with no family history and control subjects. All of the subjects were Japanese. MMD was diagnosed on the basis of guidelines established by the Research Committee on Spontaneous Occlusion of the Circle of Willis of the Ministry of Health and Welfare of Japan. This study was approved by the Ethics Committee of Tohoku University School of Medicine. Total RNA samples were purified from leukocytes using an RNeasy mini kit (Qiagen, Hilden, Germany) and used as templates for cDNA synthesis with an Oligo $(dT)_{20}$ primer and SuperScript II reverse transcriptase according to the manufacturer's instructions (Invitrogen, Carlsbad, CA, USA).

Linkage analysis

For the linkage analysis, DNA samples were genotyped for 36 microsatellite markers within five previously reported MMD loci using the ABI 373A DNA Sequencer (Applied Biosystems, Foster City, CA, USA). Pedigrees and haplotypes were constructed with the Cyrillic version 2.1 software (Oxfordshire, UK). Multipoint analyses were conducted using the GENEHUNTER 2 software (http://www.broadinstitute.org/ftp/distribution/software/genehunter/). Statistical analysis was performed with SPSS version 14.0J (SPSS, Tokyo, Japan).

Genome-wide and locus-specific association studies

A genome-wide association study was performed using a group of 72 MMD patients, which consisted of 64 patients without a family history of MMD and 8 probands of MMD families. The Illumina Human Omni-Quad 1 chip (Illumina, San Diego, CA, USA) was used for genotyping, and single-nucleotide polymorphisms (SNPs) with a genotyping completion rate of 100% were used for further statistical analysis (785 720 out of 1 140 419 SNPs). Genotyping data from 45 healthy Japanese controls were obtained from the database at the International HapMap Project web site. The 785 720 SNPs were statistically analyzed using the PLINK software (http://pngu.mgh.harvard.edu/~purcell/plink/index.shtml). For a locus-specific association study, we used 63 DNA samples consisting of 58 non-familial MMD patients and 5 probands of MMD families. A total of 384 SNPs within chromosome 17q25-ter were genotyped (Supplementary Table 1), using the GoldenGate Assay and a custom SNP chip (Illumina). Genotyping data for 45 healthy Japanese were used as a control. Case–control single-marker analysis, haplotype frequency estimation and significance testing of differences in haplotype frequency were performed using the Haploview version 3.32 program (http://www.broad.mit.edu/mpg/haploview/).

Mutation detection

Mutational analyses of *RNF213* and *FLJ35220* were performed by PCR amplification of each coding exon and putative promoter regions, followed by direct sequencing. Genomic sequence data for the two genes were obtained from the National Center for Biotechnology Information web site (http://www.ncbi.nlm.nih.gov/) for design of exon-specific PCR primers. *RNF213* cDNA fragments were amplified from leukocyte mRNA for sequencing analysis. Sequencing of the PCR products was performed with the ABI BigDye Terminator Cycle Sequencing Reaction Kit using the ABI 310 Genetic Analyzer. Identified base changes were screened in control subjects. Statistical difference of the carrier frequency of each base change was estimated by Fisher's exact test (the MMD group vs the control group).

Quantitative PCR

MTC Multiple Tissue cDNA Panels (Clontech Laboratory, Madison, WI, USA) were the source of cDNAs from human cell lines, adult and fetal tissues. Mononuclear cells and polymorphonuclear cells were isolated from the fresh peripheral blood of healthy human adults using Polymorphprep (Cosmo Bio,

Carlsbad, CA, USA). T and B cells were isolated from the fresh peripheral blood of healthy human adults using the autoMACS separator (Militeny Biotec, Bergisch Gladbach, Germany). Total RNA was isolated from these cells with the RNeasy Mini Kit (Qiagen) following the manufacturer's instructions. We reverse transcribed 100 ng samples of total RNA into cDNAs using the High Capacity cDNA Reverse Transcription Kit (Applied Biosystems). Quantitative PCRs were performed in a final volume of 20 μl using the FastStart TaqMan Probe Master (Rox) (Roche, Madison, WI, USA), 5 μl of cDNA, 10 μM of *RNF*- or *GAPDH*-specific primers and 10 μM of probes (Universal ProbeLibrary Probe #80 for *RNF213* and Roche Probe #60 for *GAPDH*). All reactions were performed in triplicate using the ABI 7500 Real-Time PCR system (Applied Biosystems). Cycling conditions were 2 min at 50°C and 10 min at 95°C, followed by 40 cycles of 15 s at 95°C and 60 s at 60°C. Real-time PCR data were analyzed by the SDS version 1.2.1 software (Applied Biosystems). We evaluated the relative level of *RNF213* mRNA by determining the C_T value, the PCR cycle at which the reporter fluorescence exceeded the signal baseline. *GAPDH* mRNA was used as an internal reference for normalization of the quantitative expression values.

Multiplex PCR

MTC Multiple Tissue cDNA Panels (Clontech) were the source of human cell lines and cDNAs from human adult and fetal tissues. Multiplex PCRs were performed in a final volume of 20 μl using the Multiplex PCR Master Mix (Qiagen), 2 μl of cDNA, a 2 μM concentration of *RNF213* and a 10 μM concentration of *GAPDH*-specific primers. The samples were separated on a 2% agarose gel stained with ethidium bromide. Cycling conditions were 15 min at 94°C, followed by 30 cycles of 30 s at 94 °C, 30 s at 57 °C and 30 s at 72 °C. For normalization of the expression levels, we used *GAPDH* as an internal reference for each sample.

In situ hybridization (ISH) analysis

Paraffin-embedded blocks and sections of mouse tissues for ISH were obtained from Genostaff (Tokyo, Japan). The mouse tissues were dissected, fixed with Tissue Fixative (Genostaff), embedded in paraffin by proprietary procedures (Genostaff) and sectioned at 6 μm. To generate anti-sense and sense RNA probes, a 521-bp DNA fragment corresponding to nucleotide positions 470–990 of mouse *Rnf213* (BC038025) was subcloned into the pGEM-T Easy vector (Promega, Madison, WI, USA). Hybridization was performed with digoxigenin-labeled RNA probes at concentrations of 300 ng ml^{-1} in Probe Diluent-1 (Genostaff) at 60 °C for 16 h. Coloring reactions were performed with NBT/BCIP solution (Sigma-Aldrich, St Louis, MO, USA). The sections were counterstained with Kernechtrot stain solution (Mutoh, Tokyo, Japan), dehydrated and mounted with Malinol (Mutoh). For observation of *Rnf213* expression in activated lymphocytes, 10-week-old Balb/c mice were intraperitoneally injected with 100 μg of keyhole limpet hemocyanin and incomplete adjuvant and sacrificed in 2 weeks. The spleen of the mice was removed for Hematoxylin–eosin staining and ISH analyses.

RESULTS

Using 20 Japanese MMD families, we reevaluated the linkage mapped previously to five putative MMD loci. No locus with significant linkage, Lod score >3.0 or NPL score >4.0 was confirmed (Supplementary Figure 2). We conducted a genome-wide association study of 72 Japanese MMD cases. Single-marker allelic tests comparing the 72 MMD cases and 45 controls were performed for 785 720 SNPs using χ^2 statistics. These tests identified a single locus with a strong association with MMD ($P<10^{-8}$) on chromosome 17q25-ter (Figure 1b), which is in line with the latest mapping data of a MMD locus.[16] The SNP markers with $P<10^{-6}$ are listed in Table 1. To confirm this observation, we performed a locus-specific association study. A total of 384 SNP markers (Supplementary Table 1) were selected within the chromosome 17q25-ter region and genotyped in a set of 63 MMD cases and 45 controls. The SNP markers demonstrating a high association with MMD ($P<10^{-6}$) were clustered in a 151-kb region from base position 75 851 399–76 003 020 (SNP No.116–136 in

Table 1 A genome-wide association study of Japanese MMD patients and controls

	SNP	Chromosome	Base position	Gene	Risk allele/ non-risk allele	Risk allele frequency in MMD	Risk allele frequency in controls	χ^2	P-value	Odds ratio	95% confidence interval	
											Lower	Upper
1	rs11870849	17	76 025 668	*RNF213*	T/C	0.4792	0.1111	33.55	6.95E-09	7.36	3.532	15.34
2	rs6565681	17	75 963 089	*RNF213*	A/G	0.7361	0.3667	31.35	2.16E-08	4.819	2.733	8.489
3	rs7216493	17	75 941 953	*RNF213*	G/A	0.75	0.3889	30.39	3.53E-08	4.715	2.673	8.313
4	rs7217421	17	75 850 055	*RNF213*	A/G	0.6667	0.3	29.86	4.64E-08	4.666	2.642	8.237
5	rs12449863	17	75 857 806	*RNF213*	C/T	0.6667	0.3	29.86	4.64E-08	4.666	2.642	8.237
6	rs4890009	17	75 926 103	*RNF213*	G/A	0.8819	0.5778	28.5	9.38E-08	5.459	2.831	10.527
7	SNP17-75933731	17	75 933 731	*RNF213*	G/A	0.8819	0.5778	28.5	9.38E-08	5.458	2.831	10.527
8	rs7219131	17	75 867 365	*RNF213*	T/C	0.6667	0.3111	28.11	1.15E-07	4.429	2.517	7.794
9	rs6565677	17	75 932 037	*RNF213*	T/C	0.7431	0.3977	27.43	1.63E-07	4.378	2.483	7.722
10	rs4889848	17	75 969 256	*RNF213*	C/T	0.75	0.4111	26.99	2.05E-07	4.297	2.444	7.889
11	rs7224239	17	75 969 771	*RNF213*	A/G	0.8681	0.5667	26.99	2.05E-07	5.03	2.659	9.529

Abbreviations: MMD, moyamoya disease; SNP, single-nucleotide polymorphism.A genome-wide association study testing 1 140 419 SNPs on the Human Omni-Quad 1chip (Illumina, San Diego, CA, USA) was performed in 72 Japanese MMD cases. Single-marker allelic tests between the cases and controls were performed using χ^2 statistics for all markers. This table lists the 11 SNP markers with a significance of $P<10^{-6}$.

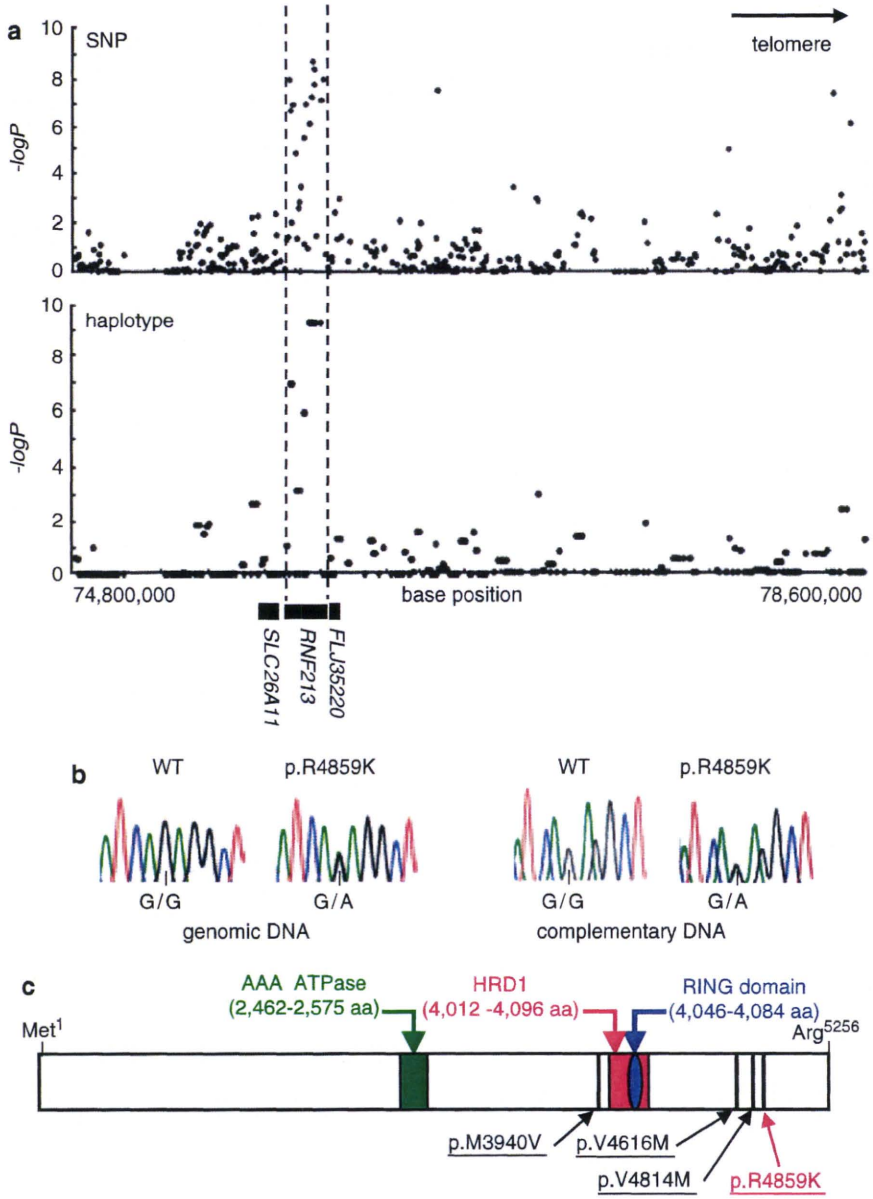

Figure 2 (**a**) Association analysis of 63 non-familial MMD cases and 45 control subjects. Statistical significance was evaluated by the χ^2-test. SNP markers with a strong association with MMD ($P<10^{-6}$) clustered in a 161-kb region (base position 75 851 399–76 012 838) indicated by two dotted lines (upper panel), which included the entire region of *RNF213* (lower panel). Haplotype analysis revealed a strong association ($P=5.3\times10^{-10}$) between MMD and a single haplotype located within *RNF213*. (**b**) Sequencing chromatograms of the identified MMD mutations. The left panel shows the sequences of an unaffected individual and a carrier of a p.R4859K heterozygous mutation. The right panel indicates the sequencing chromatograms of the leukocyte cDNA obtained from an unaffected individual and an individual with MMD who carries the p.R4859K mutation. Note that both wild-type and mutant alleles were expressed in leukocytes. (**c**) The structure of the RNF213 protein. The RNF213 protein contains three characteristic structures, the AAA-superfamily ATPase motif, the RING motif and the HMG-CoA reductase degradation motif. The positions of four mutations identified in MMD patients are underlined, including one prevalent mutation (red) and three private mutations (black).

Supplementary Table 1); this entire region was within the *RNF213* locus (Figure 2a). A single haplotype determined by seven SNPs (SNP Nos.130–136 in Supplementary Table 1) that resided in the 3′ region of *RNF213* was strongly associated with MMD onset ($P=5.3\times10^{-10}$). Analysis of the linkage disequilibrium block indicated that this haplotype was not in complete linkage disequilibrium with any other haplotype in this region (Supplementary Figure 3). These results strongly suggest that a founder mutation may exist in the 3′ part of *RNF213*.

Mutational analysis of the entire coding and promoter regions of *RNF213* and *FLJ35220*, a gene 3′ adjacent to *RNF213*, revealed that 19 of the 20 MMD families shared the same single base substitution, c.14576G>A, in exon 60 of *RNF213* (Figure 2b and Table 2). This nucleotide change causes an amino-acid substitution from arginine^{4859} to lysine^{4859} (p.R4859K). The p.R4859K mutation was identified in 46 of 63 non-familial MMD cases (73%), including 45 heterozygotes and a single homozygote (Table 3). Both the wild-type and the p.R4859K mutant alleles were co-expressed in leukocytes

Table 2 Nucleotide changes with amino-acid substitutions identified in the sequencing analysis of *RNF213* and *FLJ35220*

Gene	Exon	Nucleotide change[a] (amino-acid substitution)	Genotype (allele)		P-value[b]	χ^2 (df=1)[c]	Odds ratio (95% CI)
			Non-familial cases	Control subjects			
RNF213	29	c.7809C>A (p.D2603E)	2/63 (2/126)	15/381 (15/762)	0.77	0.09	0.80 (0.2–3.6)
RNF213	41	c.11818A>G (p.M3940V)	1/63 (1/126)	0/388 (0/776)	0.01	6.17	ND
RNF213	41	c.11891A>G (p.E3964G)	4/63 (4/126)	3/55 (4/110)	0.84	0.04	1.2 (0.3–5.5)
RNF213	52	c.13342G>A (p.A4448T)	4/63 (4/126)	2/53 (2/106)	0.53	0.39	1.7 (0.3–9.8)
RNF213	56	c.13846G>A (p.V4616M)	1/63 (1/126)	0/388 (0/776)	0.01	6.17	ND
RNF213	59	c.14440G>A (p.V4814M)	1/63 (1/126)	0/388 (0/776)	0.01	6.17	ND
RNF213	60	c.14576G>A (p.R4859K)	46/63 (47/126)	6/429 (6/858)	1.2×10^{-43}	298.1	190.8 (71.7–507.9)
FLJ35220		None					

Abbreviations: ND, not determined; SNP, single-nucleotide polymorphism.
[a]Nucleotide numbers of *RNF213* cDNA are counted from the A of the ATG initiator methionine codon (NCBI Reference sequence, NP_065965.4).
[b]*P*-values were calculated by Fisher's exact test.
[c]Genotypic distribution (carrier of the polymorphism vs non-carrier).

Table 3 Association of the p.R4859K (c.14576G>A) mutation with MMD

	Total	Genotype		
		wt/wt (%)	*wt/p.R4859K* (%)	*p.R4859K/ p.R4859K* (%)[d]
Members of 19 MMD families[a]				
Affected	42	0	39 (92.9)	3 (7.1)
Not affected	28	15 (53.6)	13 (46.4)	0
Individuals without a family history of MMD[b,c]				
Affected	63	17 (27.0)	45 (71.4)	1 (1.6)
Not affected	429	423 (98.6)	6 (1.4)	0

Abbreviations: MMD, moyamoya disease.
[a]Entire distribution, $\chi^2=29.4$, $P=4.2\times10^{-7}$.
[b]Entire distribution, $\chi^2=298.2$, $P=1.8\times10^{-65}$.
[c]Genotypic distribution (p.R4859K carrier vs non-carrier), $\chi^2=298.1$, $P=1.2\times10^{-43}$, odds ratio=190.8 (95% CI=71.7–507.9).
[d]The age of onset and initial symptoms of the four homozygotes were comparable to those of the 84 heterozygous patients.

in three patients heterozygous for the p.R4859K mutation (Figure 2b), excluding the possible instability of the mutant *RNF213* mRNA. Additional missense mutations, p.M3940V, p.V4616M and p.V4814M, were detected in three non-familial MMD cases without the p.R4859K mutation (Figure 2c). These mutations were not found in 388 control subjects and were detected in only one patient, suggesting that they were private mutations (Table 2). No copy number variation or mutation was identified in the *RNF213* locus of 12 MMD patients using comparative genome hybridization microarray analysis (Supplementary Figure 4). In total, 6 of the 429 control subjects (1.4%) were found to be heterozygous carriers of p.R4859K. Therefore, we concluded that the p.R4859K mutation increases the risk of MMD by a remarkably high amount (odds ratio=190.8 (95% confidence interval=71.7–507.9), $P=1.2\times10^{-43}$) (Table 3). It was recently reported that an SNP (ss161110142) in the promoter region of *RPTOR*, which is located ~150 kb downstream from *RNF213*, was associated with MMD.[17] Genotyping of the SNP in *RPTOR* showed that the *RNF213* p.R4859K mutation was more strongly associated with MMD than ss161110142 (Supplementary Figure 1).

RNF213 encodes a protein with 5256 amino acids harboring a RING (really interesting new gene) finger motif, suggesting that it functions as an E3 ubiquitin ligase (Figure 2c). It also has an AAA ATPase domain, which is characteristic of energy-dependent unfoldases.[18] To our knowledge, RNF213 is the first RING finger protein known to contain an AAA ATPase domain. The expression profile of *RNF213* has not been previously fully characterized. We performed a quantitative reverse transcription PCR analysis in various human tissues and cells. *RNF213* mRNA was highly expressed in immune tissues, such as spleen and leukocytes (Figure 3a and Supplementary Figure 5). Expression of *RNF213* was detected in fractions of both polymorphonuclear cells and mononuclear cells and was found in both B and T cell fractions (Supplementary Figure 6). A low but significant expression of *RNF213* was also observed in human umbilical vein endothelial cells and human pulmonary artery smooth muscle cells. Cellular expression was not enhanced in tumor cell lines, compared with leukocytes. In human fetal tissues, the highest expression was observed in leukocytes and the thymus (Supplementary Figure 6E). The expression of *RNF213* was surprisingly low in both adult and fetal brains. Overall, *RNF213* was ubiquitously expressed, and the highest expression was observed in immune tissues.

We studied the cellular expression of *Rnf213* in mice. The ISH analysis of spleen showed that *Rnf213* mRNA was present in small mononuclear cells, which were mainly localized in the white pulps (Figures 3b–g). The ISH signals were also detected in the primary follicles in the lymph node and in thymocytes in the medulla of the thymus (Supplementary Figure 7). To study *Rnf213* expression in activated lymphocytes we immunized mice with keyhole limpet hemocyanin, and examined *Rnf213* mRNA in spleen by ISH analysis. Primary immunization with keyhole limpet hemocyanin antigen revealed that the expression of *Rnf213* in the secondary follicle is as high as in the primary follicle in the lymph node (Supplementary Figure 8). In an E16.5 mouse embryo, expression was observed in the medulla of the thymus and in the cells around the mucous palatine glands (Supplementary Figure 9). These findings suggest that mature lymphocytes in a static state express *Rnf213* mRNA at a higher level than do their immature counterparts.

DISCUSSION

We identified a susceptibility locus for MMD by genome-wide and locus-specific association studies. Further sequencing analysis revealed a founder missense mutation in *RNF213*, p.R4859K, which was tightly associated with MMD onset. Identification of a founder mutation in individuals with MMD would resolve the following recurrent

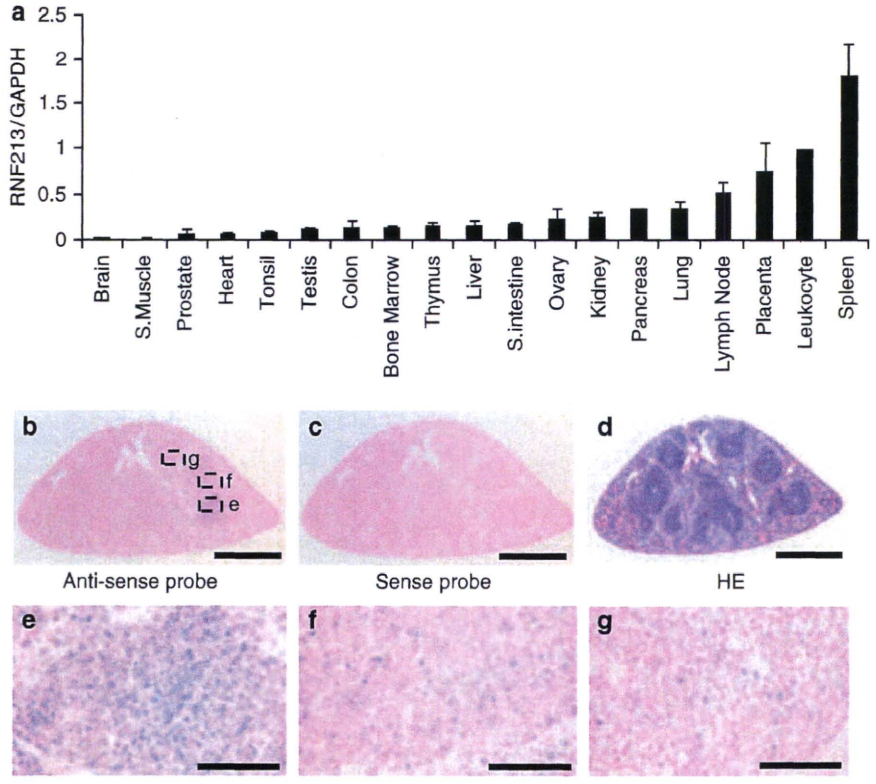

Figure 3 Expression of human RNF213 and murine Rnf213. (**a**) RT-PCR analysis of RNF213 mRNA in various human tissues. The expression levels of *RNF213* mRNA in various adult human tissues were evaluated by quantitative PCR using *GAPDH* mRNA as a control. The signal ratio of *RNF213* mRNA to *GAPDH* mRNA in each sample is shown on the vertical axis. (**b–g**) *In situ* hybridization (ISH) analysis of Rnf213 mRNA in mouse spleen. Specific signals for *Rnf213* mRNA were detected by ISH analysis with the anti-sense probe (**b**) but not with the sense probe (**c**). Hematoxylin–eosin staining of the mouse spleen (**d**). Signals for the *Rnf213* mRNA were observed in small mononuclear cells, which were mainly localized in the white pulps (dotted square, **e**) and partially distributed in the red pulps (dotted squares, **f** and **g**). Panels e, f and g show the high-magnification images of the corresponding fields in panel b. Scale bars, 1 mm (**b–d**) and 50 μm (**e–g**).

questions:[2,19] (i) why is MMD more prevalent in East Asia than in Western countries? The carrier frequency of p.R4859K in Japan is 1/72 (Table 2). In contrast, we found no p.R4859K carrier in 400 Caucasian controls (data not shown). Furthermore, no mutation was identified in five Caucasian patients with MMD after the full sequencing of *RNF213*. These results suggest that the genetic background of MMD in Asian populations is distinct from that in Western populations and that the low incidence of MMD in Western countries may be attributable to a lack of the founder *RNF213* mutation. (ii) Is unilateral involvement a subtype of MMD or a different disease?[2] We collected DNA samples from six patients with unilateral involvement and found a p.R4859K mutation in four of them (data not shown), suggesting that bilateral and unilateral MMD share a genetic background. (iii) Is pre-symptomatic diagnosis of MMD possible? In the present study, MMD never developed in the 15 mutation-negative family members in the 19 MMD families with the p.R4859K mutation (Table 3 and Supplementary Figure 1), suggesting the feasibility of presymptomatic diagnosis or exclusion by genetic testing.

How the mutant RNF213 protein causes MMD remains to be elucidated. The expression of *RNF213* was more abundant in a subset of leukocytes than in the brain, suggesting that blood cells have a function in the etiology of MMD. This observation agrees with a previous report that MMD patients have systemic angiopathy.[20] Recent studies have suggested that the postnatal vasculature can form through vasculogenesis, a process by which endothelial progenitor cell are recruited from the splenic pool and differentiate into mature endothelial cells.[21] Levels of endothelial progenitor cells in the peripheral blood are increased in MMD patients.[22] *RNF213* may be expressed in splenic endothelial progenitor cells and mutant *RNF213* might dysregulate the function of the endothelial progenitor cells. Further research is necessary to elucidate the role of *RNF213* in the etiology of MMD.

CONFLICT OF INTEREST

The authors declare no conflict of interest.

ACKNOWLEDGEMENTS

We thank all of the patients and their families for participating in this study. We also thank Dr Hidetoshi Ikeda at the Department of Neurosurgery, Tohoku University School of Medicine and Drs Toshiaki Hayashi and Reizo Shirane at the Department of Neurosurgery, Miyagi Children's Hospital, Sendai, Japan for patient recruitment. We are grateful to Ms Kumi Kato for technical assistance. This study was supported by grants from the Ministry of Education, Culture, Sports, Science and Technology, Japan and by the Research Committee on Moyamoya Disease of the Ministry of Health, Labor and Welfare, Japan.

1 Suzuki, J. & Takaku, A. Cerebrovascular 'moyamoya' disease. Disease showing abnormal net-like vessels in base of brain. *Arch. Neurol.* **20,** 288–299 (1969).
2 Suzuki, J. *Moyamoya Disease* (Springer-Verlag: Berlin, 1983).
3 Oki, K., Hoshino, H. & Suzuki, N. In: *Moyamoya Disease Update*, (eds Cho B.K., Tominaga T.) 29–34 (Springer: New York, 2010).
4 Phi, J. H., Kim, S. K., Wang, K. C. & Cho, B. K. In: *Moyamoya Disease Update*, (eds Cho B.K., Tominaga T). 82–86, (Springer: New York, 2010).
5 Yoshihara, T., Taguchi, A., Matsuyama, T., Shimizu, Y., Kikuchi-Taura, A., Soma, T. *et al.* Increase in circulating CD34-positive cells in patients with angiographic evidence of moyamoya-like vessels. *J. Cereb. Blood Flow Metab.* **28,** 1086–1089 (2008).
6 Achrol, A. S., Guzman, R., Lee, M. & Steinberg, G. K. Pathophysiology and genetic factors in moyamoya disease. *Neurosurg. Focus.* **26,** E4 (2009).
7 Scott, R. M. & Smith, E. R. Moyamoya disease and moyamoya syndrome.. *N. Engl. J. Med.* **360,** 1226–1237 (2009).
8 Kure, S. In: *Moyamoya Disease Update* (eds Cho B.K., Tominaga T.) 41–45 (Springer: Tokyo, 2010).
9 Kuriyama, S., Kusaka, Y., Fujimura, M., Wakai, K., Tamakoshi, A., Hashimoto, S. *et al.* Prevalence and clinicoepidemiological features of moyamoya disease in Japan: findings from a nationwide epidemiological survey. *Stroke.* **39,** 42–47 (2008).
10 Sakurai, K., Horiuchi, Y., Ikeda, H., Ikezaki, K., Yoshimoto, T., Fukui, M. *et al.* A novel susceptibility locus for moyamoya disease on chromosome 8q23. *J. Hum. Genet.* **49,** 278–281 (2004).
11 Nanba, R., Kuroda, S., Tada, M., Ishikawa, T., Houkin, K. & Iwasaki, Y. Clinical features of familial moyamoya disease. *Childs. Nerv. Syst.* **22,** 258–262 (2006).
12 Ikeda, H., Sasaki, T., Yoshimoto, T., Fukui, M. & Arinami, T. Mapping of a familial moyamoya disease gene to chromosome 3p24.2-p26. *Am. J. Hum. Genet.* **64,** 533–537 (1999).
13 Inoue, T. K., Ikezaki, K., Sasazuki, T., Matsushima, T. & Fukui, M. Linkage analysis of moyamoya disease on chromosome 6. *J. Child. Neurol.* **15,** 179–182 (2000).
14 Yamauchi, T., Tada, M., Houkin, K., Tanaka, T., Nakamura, Y., Kuroda, S. *et al.* Linkage of familial moyamoya disease (spontaneous occlusion of the circle of Willis) to chromosome 17q25.. *Stroke.* **31,** 930–935 (2000).
15 Wakai, K., Tamakoshi, A., Ikezaki, K., Fukui, M., Kawamura, T., Aoki, R. *et al.* Epidemiological features of moyamoya disease in Japan: findings from a nationwide survey. *Clin. Neurol. Neurosurg.* **99**(Suppl 2), S1–S5 (1997).
16 Mineharu, Y., Liu, W., Inoue, K., Matsuura, N., Inoue, S., Takenaka, K. *et al.* Autosomal dominant moyamoya disease maps to chromosome 17q25.3. *Neurology.* **70,** 2357–2363 (2008).
17 Liu, W., Hashikata, H., Inoue, K., Matsuura, N., Mineharu, Y., Kobayashi, H. *et al.* A rare Asian founder polymorphism of Raptor may explain the high prevalence of Moyamoya disease among East Asians and its low prevalence among Caucasians. *Environ. Health. Prev. Med.* **15,** 94–104 (2010).
18 Lupas, A. N. & Martin, J. AAA proteins.. *Curr. Opin. Struct. Biol.* **12,** 746–753 (2002).
19 Ikezaki, K. In: *Moyamoya disease* (eds Ikezaki K., Loftus C. M.) 43–75 (Thieme: New York, 2001).
20 Ikeda, E. Systemic vascular changes in spontaneous occlusion of the circle of Willis. *Stroke.* **22,** 1358–1362 (1991).
21 Zampetaki, A., Kirton, J. P. & Xu, Q. Vascular repair by endothelial progenitor cells. *Cardiovasc. Res.* **78,** 413–421 (2008).
22 Rafat, N., Beck, G., Pena-Tapia, P. G., Schmiedek, P. & Vajkoczy, P. Increased levels of circulating endothelial progenitor cells in patients with Moyamoya disease. *Stroke.* **40,** 432–438 (2009).

Supplementary Information accompanies the paper on Journal of Human Genetics website (http://www.nature.com/jhg)

Stroke
JOURNAL OF THE AMERICAN HEART ASSOCIATION

American Stroke Association
A Division of American Heart Association

Confirmation of an Association of Single-Nucleotide Polymorphism rs1333040 on 9p21 With Familial and Sporadic Intracranial Aneurysms in Japanese Patients

Hirokuni Hashikata, Wanyang Liu, Kayoko Inoue, Yohei Mineharu, Shigeki Yamada, Shanika Nanayakkara, Norio Matsuura, Toshiaki Hitomi, Yasushi Takagi, Nobuo Hashimoto, Susumu Miyamoto and Akio Koizumi

Stroke 2010;41;1138-1144; originally published online Apr 15, 2010;
DOI: 10.1161/STROKEAHA.109.576694
Stroke is published by the American Heart Association. 7272 Greenville Avenue, Dallas, TX 72514
 Print ISSN: 0039-2499. Online ISSN: 1524-4628

Confirmation of an Association of Single-Nucleotide Polymorphism rs1333040 on 9p21 With Familial and Sporadic Intracranial Aneurysms in Japanese Patients

Hirokuni Hashikata, MD; Wanyang Liu, MD, MPH; Kayoko Inoue, MD, MPH, PhD; Yohei Mineharu, MD, PhD; Shigeki Yamada, MD, PhD; Shanika Nanayakkara, MD; Norio Matsuura; Toshiaki Hitomi, PhD; Yasushi Takagi, MD, PhD; Nobuo Hashimoto, MD, PhD; Susumu Miyamoto, MD, PhD; Akio Koizumi, MD, PhD

Background and Purpose—Genetic factors are important determinants of intracranial aneurysm (IA). Recently, a multinational, genome-wide association study identified 3 loci associated with IA, located on 2q (rs700651), 8q (rs10958409), and 9p (rs1333040 and rs10757278). The aim of this study was to evaluate these associations.

Methods—Familial and sporadic cases were investigated. Familial cases, consisting of 96 subjects with IA, and 46 subjects of unknown status from 31 pedigrees were analyzed with the transmission disequilibrium test and linkage analysis. Associations of single-nucleotide polymorphisms (SNPs) with IA were tested in 419 sporadic IA cases and in 408 control subjects. Sequencing of *CDKN2A*, *CDKN2B*, and *CDKN2BAS* revealed additional SNPs, and their associations with IA were also tested.

Results—The transmission disequilibrium test revealed associations of 2 SNPs, rs700651 ($P=0.036$) and rs1333040 ($P=0.002$), with familial IA. Analysis of SNPs in sporadic cases revealed an allelic association of rs1333040 with IA (odds ratio=1.28; 95% CI, 1.04–1.57; $P=0.02$) but failed to show associations of rs10757278 and rs496892 with IA. We sequenced 3 candidate genes; *CDKN2A*, *CDKN2B*, and *CDKN2BAS*. All 6 index cases from IA families had the rs1333040-T allele and SNPs (rs10965215, rs10120688, and rs7341791) in *CDKN2BAS*. None of these SNPs had linkage disequilibrium with rs1333040 and was associated with IA.

Conclusions—A region between introns 7 and 15 of *CDKN2BAS* carrying the rs1333040-T allele may confer risk for IA. (***Stroke.* 2010;41:1138-1144.**)

Key Words: genetics ■ intracranial aneurysm ■ association study ■ *CDKN2BAS* ■ single-nucleotide polymorphisms

Subarachnoid hemorrhage (SAH) is fatal in ≈50% of cases, and significant disability is caused in ≈30% of cases, despite the diagnostic and therapeutic developments of the past few decades.[1,2] In Japan, the total annual mortality rate for SAH was estimated to be 22.5 per 100 000 person-years.[3] Rupture of intracranial aneurysm (IA) accounts for >90% of SAH cases.[2] Both environmental and genetic factors are associated with IA.[4,5]

To clarify the genetic component of IA, we previously conducted genetic studies by using a multiplex IA family approach. Nonparametric linkage analysis revealed 3 loci located on 17cent, 19q13, and Xp22,[6] and parametric analysis revealed a locus on 19q13.[7] On 17cent, we found *TNFRSF13B* to be a candidate gene for IA.[8] Several other studies have revealed several loci or candidate genes in different populations.[9–19]

In 2008, Helgadottir et al[20] reported that the locus tagged by rs10757278 on chromosome 9p21 is a risk factor for IA, but not for diabetes mellitus. Bilguvar et al[21] reported a multistage, genome-wide association study of European and Japanese populations and identified 3 common single-nucleotide polymorphisms (SNPs) associated with IA on chromosomes 2q, 8q, and 9p. The aim of the present study was to investigate whether these associations could be replicated in the multiplex IA families and in sporadic Japanese IA cases.

Subjects and Methods

Study Population

Subjects from 2 groups participated. The first group consisted of subjects from previously reported families and from 3 additional families: 96 cases (male n=33; female n=63) from 31 pedigrees (Figure 1). Among the 29 previously reported pedigrees,[6] some of

Received December 17, 2009; final revision received January 30, 2010; accepted February 9, 2010.

From the Departments of Health and Environmental Sciences (H.H., W.L., K.I., S.N., N.M., T.H., A.K.) and Department of Neurosurgery (H.H., Y.M., Y.T., S.M.), Kyoto University Graduate School of Medicine, Kyoto; Shiga Medical Center for Adults (S.Y.), Shiga; and National Cardiovascular Center (N.H.), Osaka, Japan.

The first 2 authors contributed equally to this report.

Correspondence to Akio Koizumi, MD, PhD, Department of Health and Environmental Sciences, Kyoto University Graduate School of Medicine, Konoe-cho, Yoshida, Sakyo-ku, Kyoto, 606-8501, Japan. E-mail Akio.Koizumi@z06.mbox.media.kyoto-u.ac.jp

***Stroke* is available at http://stroke.ahajournals.org** **DOI: 10.1161/STROKEAHA.109.576694**

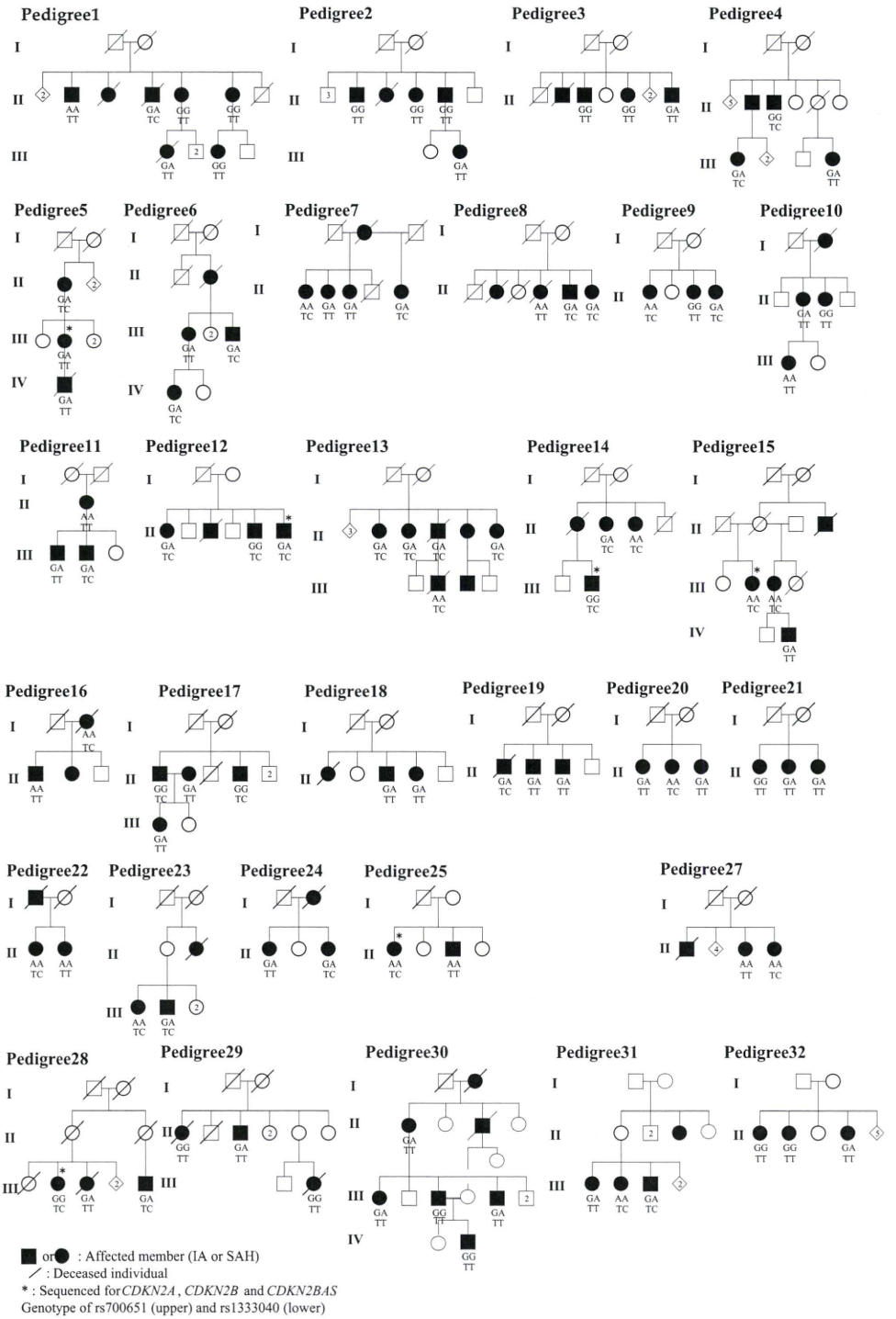

Figure 1. Pedigrees of families with IA and genotypes of individuals for rs700651 and rs1333040. Genotypes of 96 affected members are shown. Some cases have died since donating DNA samples. The identification numbers of the pedigrees are the same as previously reported.[6,8] Owing to depletion of DNA, pedigree 26 was eliminated from the figure.

the affected members could not be genotyped for rs700651, rs10958409, and rs1333040 because the DNA was exhausted by use in previous studies.

Pedigrees were recruited as previously reported.[6] In short, when cases had ≥3 living family members with IAs or ≥2 living family members with SAH, including the index cases, their families were regarded as suitable for the present study. The index cases were confirmed to have saccular aneurysms from medical records. Clinical interview and screening by magnetic resonance angiography was performed in all available relatives age 30 years or older. In subjects suspected to have IAs large enough for clinical intervention, an additional examination (digital subtraction angiography or 3-dimensional computed tomography angiography) was conducted. In addition, 46 pedigree subjects (male n=24; female n=22) who did not meet the original inclusion criteria for genetic analysis because of their young age or phenotypic uncertainty were genotyped for the current study.

The second group consisted of 419 sporadic unrelated cases (male n=142; female n=277) and 408 unrelated controls (male n=196; female n=212) collected from several collaborative hospitals in

Japan. Sporadic cases were diagnosed by digital subtraction angiography or were confirmed to have IAs during surgery. Control subjects met the following criteria: (1) confirmation of the absence of IA by digital subtraction angiography, magnetic resonance angiography, or 3-dimensional computed tomography angiography; (2) an age at examination of ≥40 years; (3) no medical history of any stroke, including IA or SAH; and (4) no family history of IA or SAH in first-degree relatives.

For all affected participants, except the 46 newly genotyped subjects, past history, lifestyle (current smoking habit and drinking habit), and comorbidity were examined from clinical records or from questionnaires conducted during interview, as previously reported.[6] For the 46 newly genotyped subjects, only their ages and relationships within pedigrees were known, whereas their IA status, comorbidities, and lifestyles were unexplored. The participation of these individuals was expected to provide greater genotype certainty in the family studies. We excluded cases or families with autoimmune diseases (including systemic lupus erythematosus, rheumatoid arthritis, and Takayasu arteritis) or known heritable diseases (including Ehlers-Danlos syndrome type IV, Marfan syndrome, neurofibromatosis type 1, and autosomal-dominant polycystic kidney disease).

This study was approved by the ethics committee of the Kyoto University institutional review board, and appropriate informed consent was obtained from all subjects.

Genotyping

We performed genotyping of 8 SNPs (rs700651, rs10958409, rs496892, rs10965215, rs10120688, rs1333040, rs7341791, and rs10757278) by using the polymerase chain reaction invader assay with TaqMan probes (Applied Biosystems TaqMan SNP genotyping assays, Foster City, Calif). The rationale for selecting the 9p SNP set, rs496892, rs1333040, and rs10757278, was the linkage disequilibrium (LD) structure of SNPs on 9p21.3. The LD block can be divided into 2 major blocks: 1 associated with vascular diseases (vascular disease block) and 1 with diabetes mellitus (diabetes block).[20] The SNPs selected are in the vascular disease block.[20–22] The physical distances between rs496892 and rs1333040 and between rs1333040 and rs10757278 are 59 and 41 kb, respectively. rs10965215, rs10120688, and rs7341791 were selected on the basis of the sequencing results of cyclin-dependent kinase inhibitor 2B antisense RNA (*CDKN2BAS*).

Linkage Analysis and Transmission Disequilibrium Test for IA Pedigrees

Two-point nonparametric logarithm of the odds scores were calculated with GENEHUNTER (version 2.1_r6)[23] for 3 SNPs (rs700651, rs10958409, and rs1333040) in the 96 affected members and in the 46 newly genotyped subjects with a disease frequency of 0.001, a phenocopy frequency of 0.02, and a penetrance of 0.70.[6] Allele frequencies of markers were set at those in controls.

To test for association of SNPs with the familial IA phenotype, we conducted the transmission disequilibrium test with TDTae software developed by Gordon et al.[24] We selected GHLO (Gordon Heath Liu Ott) error model parameters without setting the mode "inheritance."[25] In these analyses, phenotype was treated as "unknown" for the 46 newly genotyped subjects.

Association Study of SNPs With IA

An association study was performed on the 419 sporadic unrelated cases and 408 unrelated control subjects wit the SNP&Variation suite v7 (Golden Helix Inc, available at http://www.goldenhelix.com/) with or without adjustment for covariates, including sex, age, current smoking habit, and hypertension. D′ and r^2 values were also calculated for SNPs around rs1333040. Statistical power was estimated with a power calculator (available at http://pngu.mgh.harvard.edu/≈purcell/gpc/cc2.html).[26] The statistical power of the present study was 76% for $\alpha=0.05$ when the frequency of the risk allele was 0.3 with a relative risk of 1.5 when D′=0.9 for a genetic marker.

Table 1. Characteristics of Familial Cases, Sporadic Cases, and Controls

Characteristic	Familial Cases	Sporadic Cases	Controls	*P*
Subjects, n, male: female	96 (33:63)	419 (142:277)	408 (196:212)	0.000086*
Cases per pedigree, mean±SD	3.10±1.13			
Age, mean±SD, y	60.5±13.6	60.0±10.7	62.0±10.1	0.025†
Cases with SAH, n (%)	60 (62.5%)	241 (57.5%)		0.37*
Subjects with hypertension, n (%)	39 (40.6%)	215 (51.3%)	162 (39.7%)	0.0024*
Subjects currently smoking, n (%)	37 (38.5%)	151 (36.0%)	161 (39.5%)	0.59*

*Comparison among familial cases, sporadic cases, and controls was made by the χ^2 test.

†Comparison was made by ANOVA.

Sequencing Candidate Genes

Three genes, *CDKN2A*, *CDKN2B*, and *CDKN2BAS*, which are in the vicinity of rs1333040, were selected for sequencing in 6 arbitrarily selected index cases from the 31 families with IA. Six index cases were selected before initiation of this study without any biases from the genotyping results. For *CDKN2A* and *CDKN2B*, we conducted direct sequencing of all coding exons, putative promoter sequences (2 kb upstream from the initiation codon), and 100 bp on either side of intron-exon boundaries. For *CDKN2BAS*, we sequenced 19 exons and 100 bp on either side of intron-exon boundaries.

For analyses, we referred to genes on the NCBI MapViewer (build 37.1, available at http://www.ncbi.nlm.nih.gov/mapview/) and to HapMap-JPT (International HapMap Project, available at http://www.hapmap.org). After polymerase chain reaction amplification and purification, samples were run on an ABI Prism 3100 Avant DNA sequencer (Applied Biosystems). Primers are summarized in supplemental Table I (available online at http://stroke.ahajournals.org). We checked sequences against the SNP database (available at http://www.ncbi.nlm.nih.gov/SNP/index.html).

Statistical Analysis

We conducted statistical analysis with SNP&Variation suite v7 software (Golden Helix Inc). Multiple comparisons were not corrected. A nominal $P<0.05$ was considered significant. Proportions were compared by the χ^2 test, and means were compared by ANOVA with SAS software (version 8.2; SAS Institute Inc, Cary, NC).

Results

Demographic Characteristics of the Study Population

Demographic data of the study population are shown in Table 1. For familial cases, an average of 3.10±1.13 (ie, mean± SD) cases (range, 2 to 7 cases) per family was included in this study (Figure 1). The proportions of female cases and of those with hypertension were different among the 3 groups ($P<0.05$), whereas the proportion of cases with a current smoking habit was not different. Hypertension was more prevalent in sporadic cases, and the proportion of females was significantly greater in the control group. No significant difference between groups was found in the proportion of cases with SAH (Table 1). To avoid confounding effects from

Table 2. Significant Associations of rs700651 and rs1333040 With IA in 31 Pedigrees, Assessed by the TDT

SNP	Position	*P* for TDT	NPL Score	*P* for NPL
rs700651 (A/G)	2q33.1	0.036	−0.212	0.571
rs10958409 (G/A)	8q11.12–12.1	0.962	−0.605	0.72
rs1333040 (C/T)	9p21.3	0.002	−0.434	0.658

TDT indicates transmission disequilibrium test; NPL, nonparametric logarithm of the odds.

known risk factors (female sex, age, and hypertension), we adjusted for these factors in the association study.

Transmission Disequilibrium Test for SNP Association With IA in Familial Cases

The transmission disequilibrium test revealed significant associations of rs700651 (P=0.036) and rs1333040 (P=0.002; Figure 1 and Table 2) with IA, whereas the association of rs10958409 with IA was not significant (P=0.962). Nonparametric logarithm of the odds scores indicated that none of the SNPs were significantly linked with IA (Table 2).

Association of SNPs With IA in Sporadic Cases

We then investigated the association of rs700651, rs10958409, rs496892, rs1333040, and rs10757278 with IA in sporadic cases. A significant association of rs1333040 with IA was shown by allelic association (P=0.02) and by the additive model (P=0.04), whereas associations of the other SNPs were not significant (Table 3). SNPs rs496892, rs1333040, and rs10757278 were not in strong LD in the study population (Figure 2). The allele frequencies of the risk allele rs1333040-T in controls and in cases were 0.64 and 0.70, respectively. These values are similar to those reported in Japanese subjects (controls:cases=0.65:0.72), but the value for cases is larger than that reported for white subjects (controls:cases=0.47:0.52 in Finland and 0.55:0.62 in the Netherlands).[21]

Sequence Analysis of *CDKN2A*, *CDKN2B*, and *CDKN2BAS*

rs1333040 is located deep in the 12th intron of *CDKN2BAS*; therefore, we searched for more substantial genomic variants than rs1333040. *CDKN2A* and *CDKN2B* are reported to be associated with cell proliferation, aging, senescence, and apoptosis,[27] and the transcriptional regulation of *CDKN2BAS* is coordinated with that of *p16/CDKN2A* and *p15/CDKN2B*.[28] Therefore, we investigated whether 6 index cases from IA families harbor mutations in these genes. Sequencing failed to show new polymorphic variants in the coding regions of *CDKN2A* and *CDKN2B*. In contrast, several polymorphisms were found in *CDKN2BAS* (Table 4). It is of interest that a common haplotype was shared by the 6 index cases, who carry the rs1333040-T allele. Because rs10965215-A, rs10120688-A, and rs7341791-G were on the same haplotype, we investigated the associations of these 3 SNPs with IA. These SNPs, however, did not show either LD with rs1333040 (Figure 2) or association with IA (Table 3), indicating a possibility that the core risk haplotype is located between introns 7 and 15 of *CDKN2BAS*. The LD block for cases did not differ from that for controls (data not shown).

Discussion

Many studies have been performed to identify IA susceptibility gene(s).[6,9–14] Some loci have been confirmed but others have not.[19] Difficulties inherent in the identification of genetic risk factors are considered to be associated with population stratification, confounding nongenetic factors, or both.[29] To overcome such difficulties, large-scale studies

Table 3. Analysis of 8 SNPs for Association With IA in a Case-Control Study

SNPs	Allele, *d*/*D**	Groups	Genotype (No. of Subjects) *dd*	*dD*	*DD*	Risk Allele Frequency	HWE, *P*†	Allelic Association† OR (95% CI)/*P*	Genotype Association Models§ Additive OR (95% CI)/*P*	Dominant OR (95% CI)/*P*	Recessive OR (95% CI)/*P*
rs700651	A/G	Case	112	208	99	0.48	0.90	1.09 (0.90–1.32)	1.14 (0.94–1.39)	1.24 (0.91–1.70)	1.14 (0.82–1.59)
2q33.1		Control	122	194	92	0.46	0.38	0.39	0.19	0.18	0.44
rs10958409	G/A	Case	236	155	28	0.25	0.71	0.86 (0.69–1.07)	0.85 (0.67–1.06)	0.78 (0.59–1.04)	0.95 (0.55–1.66)
8q11.12–12.1		Control	208	170	30	0.28	0.56	0.17	0.15	0.09	0.86
rs496892	A/G	Case	51	179	189	0.66	0.39	1.01 (0.83–1.24)	1.02 (0.83–1.26)	0.87 (0.56–1.35)	1.10 (0.83–1.46)
9p21.3		Control	44	188	176	0.66	0.55	0.90	0.84	0.54	0.51
rs10965215	G/A	Case	51	180	188	0.66	0.44	1.00 (0.81–1.22)	1.01 (0.82–1.25)	0.88 (0.57–1.37)	1.07 (0.81–1.42)
9p21.3		Control	44	186	178	0.66	0.66	0.97	0.92	0.58	0.62
rs10120688	G/A	Case	51	172	196	0.67	0.17	1.03 (0.84–1.26)	1.04 (0.85–1.28)	0.90 (0.58–1.40)	1.12 (0.85–1.49)
9p21.3		Control	45	182	181	0.67	0.94	0.78	0.70	0.65	0.42
rs1333040	C/T	Case	36	180	203	0.70	0.66	1.28 (1.04–1.57)	1.25 (1.01–1.55)	1.55 (0.98–2.46)	1.26 (0.95–1.67)
9p21.3		Control	51	187	170	0.65	0.97	0.02	0.04	0.06	0.11
rs7341791	A/G	Case	45	169	205	0.69	0.25	1.12 (0.91–1.38)	1.13 (0.92–1.39)	1.29 (0.84–2.00)	1.13 (0.86–1.50)
9p21.3		Control	52	169	187	0.67	0.16	0.27	0.24	0.25	0.38
rs10757278	A/G	Case	100	196	123	0.53	0.21	1.15 (0.95–1.39)	1.19 (0.98–1.45)	1.31 (0.95–1.80)	1.23 (0.90–1.69)
9p21.3		Control	112	192	104	0.49	0.24	0.14	0.08	0.11	0.19

*Allele *D* indicates risk alleles; *d*, wild-type alleles; and OR, odds ratio.

†*P*, HWE, 2-sided probability value from testing for deviation from Hardy-Weinberg equilibrium.

‡Without adjustment for covariates.

§With adjustment for sex, age, hypertension, and current smoking habit.

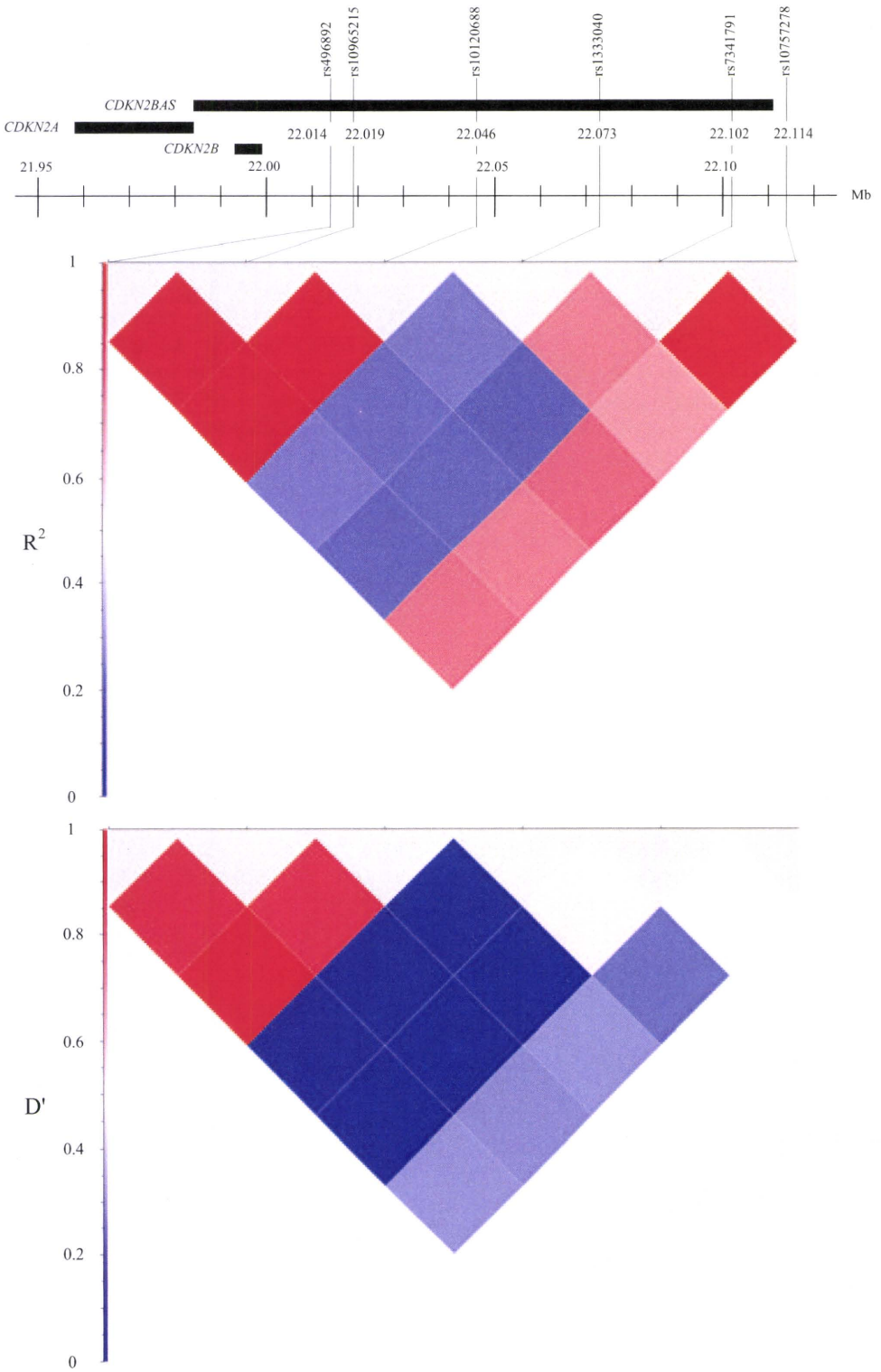

Figure 2. Six selected SNPs on 9p21.3 and LD blocks. Physical positions of 6 SNPs and related genes are illustrated, based on the NCBI database (build 37.1). LD blocks are shown by D′ and r^2 measures for a population including both cases and controls.

have been undertaken. Helgadottir et al[20] and Bilguvar et al[21] reported association studies based on a multiethnic population. Helgadottir et al[20] reported that rs10757278 (9p21) was associated with IA and that its association was independent of the diabetes block. On the other hand, Bilguvar et al[21] revealed a set of SNPs, rs700651 (2q33), rs10958409 (8q11), and rs1333040 (9p21), associated with IA.

We confirmed an association of rs1333040 with IA in 2 independent patient groups with a high or low likelihood of genetic predisposition: the multiplex IA families and sporadic cases, respectively. Such associations of rs1333040-T with IA in 2 independent populations are firmly suggestive of a substantial association with IA. To search for the gene on 9p modifying the risk of IA, we sequenced 3 genes in the vicinity

Table 4. Sequence Variants of *CDKN2A*, *CDKN2B*, and *CDKN2BAS* in Index Cases From IA Families

Gene, Nucleotide No. (Physical Position)	Position†	SNP	Description	Reference Sequence	Sequence Variants					
					Pedigree 5	Pedigree 12	Pedigree 14	Pedigree 15	Pedigree 25	Pedigree 28
CDKN2A		None								
NT_008413.17										
(21984489–21957750)										
CDKN2B		None								
NT_008413.18										
(2199931 1–21992901)										
CDKN2BAS	22019445	rs10965215*	Ex2	G	AA	AA	AA	AA	AA	AA
NT_008413.18	22036493	Unregistered	IVS4	A	AA	AA	AA	AA	AA	AC
(21984549–22111095)	22039130	rs10738605	Ex6	C	GG	GG	GG	GG	GG	GG
	22046295	rs7853090	Ex7	T	CC	CC	CC	CC	CC	CC
	22046359	rs7866783	Ex7	A	GG	GG	GG	GG	GG	GG
	22046499	rs10120688*	IVS7	G	AA	AA	AA	AA	AA	AA
	22052134	rs1011970	IVS9	G	GG	GG	GG	GG	GG	GT
	22055657	rs1333039	IVS10	G	CC	CC	GC	GC	CC	CC
	22056363	rs4977755	IVS12	T	AA	AA	AA	AA	AA	AA
	22086417	Unregistered	Ex13	T	TC	TT	TT	TT	TT	TT
	22102241	rs7341786	IVS14	A	CC	AC	AC	AC	AC	AC
	22102427	rs7341791*	IVS15	A	GG	AG	AG	AG	AG	AG
	22110371	Unregistered	Ex18	G	GG	GA	GG	GA	GG	GG
	22110490–22110491	rs67452501	IVS18 (insT)	−/−	ins/ins	−/ins	−/ins	−/−	−/ins	−/ins
	22110798–22110800	rs71949643	Ex19 (delCAT)	−/−	del/del	del/del	del/del	del/del	del/del	del/del

Ins indicates insertion del; deletion.
*SNPs used for genotyping.
†According to the NCBI MapViewer (build 37.1).

of rs1333040: *CDKN2A*, *CDKN2B,* and *CDKN2BAS*. Genetic transmission suggests that a haplotype shared by 6 index cases carries the risk allele of rs1333040-T. Three SNPs (rs10965215, rs10120688, and rs7341791), however, did not demonstrate either an association or LD with rs1333040, suggesting that a region carrying the rs1333040-T allele between introns 7 and 15 of *CDKN2BAS* may confer a bona fide risk for IA.

The 9p21 locus is associated not only with vascular diseases but also with diabetes mellitus.[20] The LD structure of this locus was investigated rigorously by Helgadottir et al[20] and was found to be composed of 2 separate LD blocks: vascular disease and diabetes blocks. The vascular disease block was tagged by SNPs, rs10757278 or rs1333040, which are in strong LD. The present study, however, failed to show a strong LD for these SNPs in the Japanese population. In the current population, IA was associated with rs1333040 but not with rs4496892 or rs10757278. More important, the current study suggests the possibility of another small LD block between introns 7 and 15 of *CDKN2BAS,* which is tagged by rs1333040.

There are several limitations of this study. The major limitations are the size and single ethnicity of the study population. Although we could not detect an association of the other 7 SNPs with IA in sporadic cases, this might have been due to insufficient statistical power because of the limited size of the study population. The limited statistical power, with a maximum sensitivity of 76%, may have failed to detect associations of other SNPs with IA, including rs10757278. In addition, we did not correct for multiple comparisons in the association studies. Another limitation was the inability to provide a biological explanation for the locus associated with IA. We could not evaluate, either directly or indirectly, any functional effect of *CDKN2BAS* with respect to IA. A major strength of the study, however, was elucidation of the fine structure of the LD block in the vicinity of rs1333040.

In conclusion, we succeeded in replicating the association of rs1333040 on 9p21 with IA in 2 independent IA patient groups and suggest that the region between introns 7 and 15 of *CDKN2BAS* may be a risk modifier. Further study is needed to elucidate the biological mechanism of this association.

Acknowledgments

We are grateful to the family members for their cooperation in this study. We thank Dr Sumiko Inoue (Suzuka University of Medical Science) for technical assistance and Katsunobu Takenaka (Takayama Red Cross Hospital) and Kazuhiko Nozaki (Shiga University of Medical Science) for patient recruitment and help in magnetic resonance angiography examinations.

Sources of Funding

This work was supported by a grant from the Ministry of Education, Science, Sports, and Culture of Japan to A.K. (Tokutei Kenkyu: